

# Nonlinear Analysis of the 2<sup>nd</sup> Order Digital Phase Locked loop

Brian Daniels\* and Ronan Farrell\*\*

*Institute of Microelectronics and Wireless Systems*

*Department of Electronic Engineering,*

*National University of Ireland Maynooth,*

*E-mail: \*bdaniels@eeng.nuim.ie, \*\*rfarrell@eeng.nuim.ie*

**Abstract**— This paper proposes a rigorous stability criterion for the 2<sup>nd</sup> order digital phase locked loop (DPLL), with a charge pump phase frequency detector (CP-PFD) component. The Stability boundary is determined using piecewise linear methods to model the non-linear nature of the CP-PFD component block. It calculates the control voltage, after a predetermined number of input reference signal sampling periods, to a small initial voltage offset. Using this piecewise linear model an exact closed form stability criterion is proposed for the second order system. The 2<sup>nd</sup> order stability boundaries, as defined by the proposed technique, are compared to that of existing linear theory stability boundaries, and display a significant improvement.

**Keywords** –Phase Locked Loop, Piecewise Linear, Stability Boundary.

## I INTRODUCTION

The Digital Phase Locked Loop (DPLL) is a versatile component block widely used in electronics for operations such as frequency synthesis and clock data recovery. The DPLL system considered in this paper consists of a bang bang phase frequency detector (PFD), a charge pump (CP), and a voltage controlled oscillator (VCO), all of which are vital to the operation of the DPLL. The DPLL may also include a low pass loop filter (LF) or a frequency divider, with a structure as shown in figure 1.

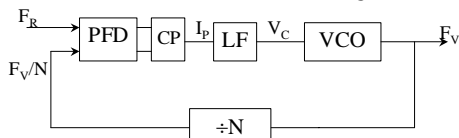


Figure 1. DPLL Loop Block Diagram

The DPLL loop generates a robust signal at the output of the VCO from a local oscillator reference signal, with a VCO output frequency  $F_v$ , that is some multiple of the reference frequency,  $F_R$ . The phase of the reference and feedback signals are compared by the PFD and any difference is represented as a current on the charge pump output,  $I_p$ . This error drives the VCO output signal towards that of the reference, and thus drives the loop towards lock.

This paper aims to determine an alternative, more accurate, stability boundary for the 2<sup>nd</sup> order system. To achieve this, the nonlinearity of the DPLL loop needs to be considered. The nonlinearities exist in the CP-PFD and the VCO component blocks. The VCO can be assumed to be linear if the DPLL system operates away from the saturation regions of

the VCO. The non-linearity in the PFD is due to quantization-like effects at the output of the PFD. This non-linearity is inherent to the operation of the loop and cannot be ignored if an accurate model is required.

Nonlinear systems are often linearised so as to ease analysis. In the case of the DPLL this can be justified if the time-varying nature of the PFD is overlooked. This is a reasonable approximation when considering the PLL to be close to lock. In this situation it's key state variable, the VCO control voltage, changes by only a small amount on each cycle of the reference signal. This is known as the continuous time approximation and is valid when the loop bandwidth is small relative to the reference frequency, or more specifically no greater than 1/10<sup>th</sup> of the reference frequency [1]. This assumes that the detailed behaviour of the loop within each cycle is not important and only the average behaviour over many cycles is important. By applying an averaged analysis, the time-varying operation can be bypassed and linear analysis can be applied. The DPLL system of figure 1 is approximated by the linear system block diagram as shown in figure 2.

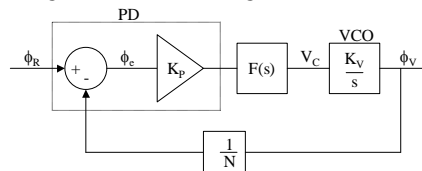


Figure 2. Linear PLL (LPLL) system

The feedback frequency divider is used in frequency synthesis to produce an output signal frequency that is some multiple of the reference signal,  $N$  times  $F_R$

in figure 1. The inclusion of a feedback divider scales  $F_V$  by  $N$ . In our analysis the divider introduces a scaling factor, however in this paper the feedback divide ratio is chosen to be equal to 1 for clarity. The transfer function of the LPLL system of figure 2 is then given by:

$$H_{CL}(s) = \frac{K_V I_p F(s)}{2\pi s + K_V I_p F(s)} \quad (1)$$

where  $I_p$  is the charge pump current gain and is equivalent to  $K_p/2\pi$ ,  $K_V$  is the VCO gain and  $F(s)$  is the loop filter transfer function. Using (1), Gardner identifies the stability boundary for the 2<sup>nd</sup> order PLL system to be:

$$K' = \frac{1}{\frac{\pi}{\omega_R \tau_2} \left( 1 + \frac{\pi}{\omega_R \tau_2} \right)} \quad (2)$$

A plot of the stability boundary from equation (2) for a defined filter time constant  $\tau_2$ , and a range of reference frequencies ( $\omega_R$  radians/2<sup>nd</sup>) is shown in figure 3.

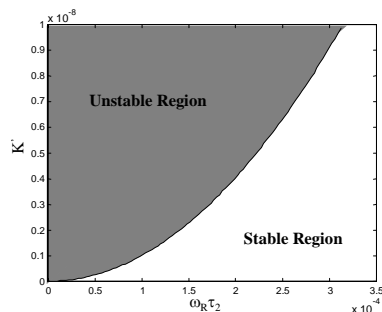


Figure 3. 2<sup>nd</sup> order Gardner Stability Boundary

Unlike Gardner [1] other linear stability criteria such as [2-4], do not provide a global prediction of the DPLL stability boundary. Instead they offer specific system parameter values from a chosen loop performance, such as the settling time [2], the phase margin [3], or the un-damped natural frequency and damping factor [4]. These linear methods ignore the nonlinearities inherent in the CP-PFD, however they do provide a starting point from which empirical design methods are used to choose optimum component values and to insure that the DPLL will operate as expected. Alternative nonlinear stability methods are unwieldy and further complicate the design of an already complex system. For this reason non-linear methods have only rarely been applied to the design of PLL systems [5-8].

The methodology proposed in this paper does not linearise the CP-PFD and thus determines a more accurate prediction of the DPLL stability boundary, allowing for more aggressive design. It uses piecewise linear methods to accurately model the inherent non-linear nature of the CP-PFD, this piecewise linear method is considered in the next section. In section III a closed form solution of the stability criterion is determined. In section IV this

stability criterion is used to plot the stability boundary of the DPLL. This boundary is compared to that of the linear model defined boundary of Gardner [1]. In section V the conclusions are presented.

## II SECOND ORDER PIECEWISE LINEAR MODEL

In this section a piecewise linear model is proposed. The proposed methodology considers the non-linearity of the CP-PFD, by using a state transition diagram to model the changing states of the CP-PFD. It assumes a small initial VCO control voltage offset  $V_0$  and determines the system stability from the state space response to this offset.  $V_0$  is chosen to be small for two reasons. First the error introduced by the model is directly proportional to  $V_0$ , and 2<sup>nd</sup> a small  $V_0$  ensures that the maximum phase offset remains within the  $\pm \pi$  region, avoiding cycle slip events. Cycle slips occur when the feedback signal falling edge, to which the reference signal falling edge is being compared to in the PFD, changes incurring a  $2\pi$  shift in the phase error. These phenomena occur when the system is substantially out of lock and in acquisition mode. Cycle slip events can be explained by this analysis but are beyond the scope of this paper.

In figure 4 a plot of the state space system trajectory is shown, where the two state variables are the phase error  $\phi_e$  and the control voltage  $V_C$ . For a stable system with a reference frequency equal to the VCO free running frequency  $F_{FR}$ , and an initial control voltage offset of  $V_0$ , the system will settle to the equilibrium of the origin, shown as the dashed line in figure 4.

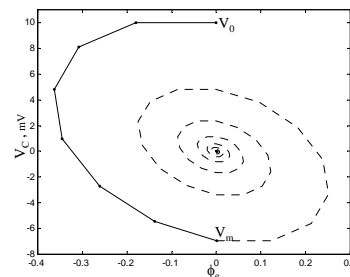


Figure 4. State Space Plot of Stable System

The continuous curve in figure 4 is a piecewise linear curve where the dots correspond to samples of the VCO control voltage. In the case of the 2<sup>nd</sup> order DPLL, the system is linear between these sample points, allowing the piecewise linear method to give an exact calculation of this state space curve. The continuous line of figure 4 is one half cycle of the state space curve. If the value of  $V_m$ , which is the first zero crossing of  $\phi_e(t)$ , can be calculated, then the system stability can be determined as follows: if  $|V_m| > V_0$  then the system trajectory is diverging and is

therefore unstable; If  $|V_m| < V_0$  then the trajectory is converging and is stable. The calculation of  $\phi_e(t)$  and  $V_C(t)$  depends on the filter's charge approximated difference equations. For the 2<sup>nd</sup> order system  $\phi_e(t)$  and  $V_C(t)$  are determined using the set of difference equations (3) and (4).

$$V_C(t_{n+1}) = V_C(t_n) - \frac{I_p T_B}{C_2} \quad (3)$$

$$\phi_e(t_{n+1}) = \phi_e(t_n) + 2\pi \left( T(F_R - F_{FR}) - \left( K_V \int V_C dt \right) \right) \quad (4)$$

where  $F_{FR}$  is the VCO free running frequency, and  $K_V$  is the VCO gain,  $T$  is the reference signal time period, and  $T_B$  is defined here as the boost time of the CP-PFD or the length of time during each period  $T$  where the CP-PFD pumps a non zero current into the loop filter. To further clarify consider one time period,  $T$ , of the loop. In this time period the DPLL operates in the coast state, where no current is output from the CP-PFD, for a period of time defined here as  $T_C$ , and in boost state for a period of  $T_B$ , as in figure 5.  $T_B$  is calculated as in equation (5).

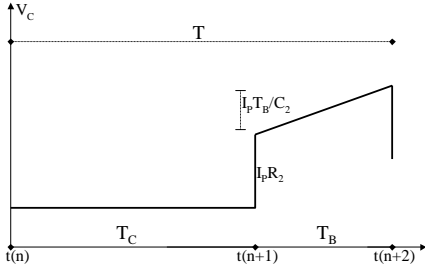


Figure 5. One Period of  $V_C$  for 2<sup>nd</sup> Order DPLL

$$T_B = \left| \frac{\phi_e(t_n) T}{2\pi} \right| \quad (5)$$

where  $\phi_e(t_n)$  is the phase error at time  $t_n$ . The coast time period is calculated as  $T_C = T_B - T$ . Once the time periods are calculated,  $V_C$  can be determined using (3). To solve equation (4) an estimate of the integral of  $V_C$  is required. For the 2<sup>nd</sup> order DPLL, the loop filter is first order, and therefore the integration corresponds to a linear ramp and can be expressed as:

$$\int V_C dt = T V_C(t_n) + T_B I_p R_2 + \frac{T_B^2 I_p}{2C_2} \quad (6)$$

Using this piecewise linear methodology it is possible to determine the stability boundaries for any DPLL system by solving the system equations, for a small initial VC offset and an initial  $\phi_e(t_n)$  equal to zero, by looking at the system trajectory over a short period of time as shown in figure 4. Extending this it is possible to determine a closed form stability criterion for the 2<sup>nd</sup> order system by extending. This is considered in the next section.

### III CLOSED FORM SECOND ORDER STABILITY CRITERION

In this section a more detailed consideration of the 2<sup>nd</sup> piecewise linear model is given. This approach determines the 2<sup>nd</sup> order DPLL control voltage after  $m$  periods of the reference signal,  $V_m$ , as defined in figure 4. The solution of  $V_m$  is used to define a closed form solution of the DPLL stability boundary for the 2<sup>nd</sup> order system.

To determine  $V_m$  two things need to be considered: first, when all parameters are known, the  $n^{\text{th}}$  sample of the control voltage  $V_n$  needs to be calculated in closed form; and 2<sup>nd</sup> the number of samples  $m$  needs to be calculated where  $V_m$  is the control voltage at the first zero crossing of the phase error as shown in figure 4. These two requirements are considered in the following two subsections.

#### a) Calculation of $V_n$

The 2<sup>nd</sup> order system, described by equations (3), and (4) can be reduced to the pair of summations given in (7) and (8), where  $V_0$  is an initial positive  $V_C$  offset, the initial  $\phi_e$  offset is zero, and  $\phi_e$  is always negative as in figure 4.

$$V_C(j) = V_0 + \frac{I_p T}{2\pi C_2} \sum_{i=0}^{j-1} \phi_e(i) \quad (7)$$

$$\phi_e(j) = -2\pi K_V T \sum_{i=0}^{j-1} V_C(i) \quad (8)$$

Equations (7) and (8) may be combined to give:

$$V_n = V_0 - \frac{K_V I_p T^2}{C_2} \sum_{i=0}^{n-1} \sum_{k=0}^{i-1} (1 - K_V I_p R_2 T)^{i-j-1} V_C(k) \quad (9)$$

where  $V_n$  is equivalent to  $V_C(n)$  and is an exact calculation of the control voltage after  $n$  samples. The double summation in equation (9) can be solved by either numerical iteration, or by solving a closed form simplification. This closed form solution is considered later in subsection 3.

The control voltage at the zero crossing,  $V_m$  will not correspond exactly with  $V_n$ , as the last sample  $n$  will not fall exactly on the phase error zero crossing, but will cross that line by some value  $d$ , as shown in figure 6. If samples  $n-1$  and  $n$  are both known then it is possible to calculate the value of  $V_m$  by using a linear interpolation (10).

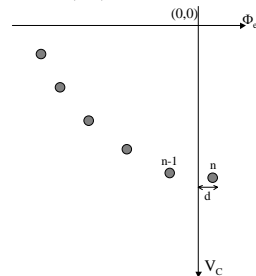


Figure 6. State Space Samples

$$V_m = V_y - \phi_y \frac{|V_x| - |V_y|}{|\phi_x| + |\phi_y|} \quad (10)$$

where  $(V_x, \phi_x)$  and  $(V_y, \phi_y)$  are the co-ordinates of the samples  $n$  and  $n-1$  respectively in figure 6. However (10) is not used in this model as the error introduced in the calculation of  $V_m$  is minimal and reduces as the reference frequency is increased.

### b) Calculation of number of samples $m$

To calculate the number of samples  $m$  it is necessary to return to the linear approximation model and use the linear error transfer function:

$$H_e(s) = \frac{C_2 s^2}{C_2 s^2 + K_V I_P R_2 C_2 s + K_V I_P} \quad (11)$$

Using linear theory to determine  $m$  does not reduce the accuracy of this technique, as we only require an approximate value of  $m$  and then round it up to the next integer. To determine the phase error zero crossings the frequency step response of (11) is calculated and the inverse Laplace taken as shown in (12) and equated to zero.

$$L^{-1} \left( \frac{2\pi \Delta_F}{s^2} H_e(s) \right) = 0 \quad (12)$$

where  $\Delta_F$  is the frequency step size. Solving (12) gives an equation of the form  $A(t) \sin(X(t)) = 0$ , which is zero when  $X(t) = 0, \pi, 2\pi, 3\pi, \dots$ . The first zero crossing after  $t = 0$  occurs when  $X(t) = \pi$ . Solving this gives equation (13), the time of the first zero crossing.

$$t_m = \frac{2\pi}{\sqrt{(K_V I_P (4 - K_V I_P R_2^2 C_2)) / C_2}} \quad (13)$$

The number of samples in one half cycle of the state space trajectory, (the solid arc of the system trajectory in figure 4) is estimated as:

$$m = \lceil t_m F_R + 1 \rceil = \left\lceil \frac{2\pi F_R}{\sqrt{(K_V I_P (4 - K_V I_P R_2^2 C_2)) / C_2}} + 1 \right\rceil \quad (14)$$

### c) Closed Form Solution of $V_m$

The value of  $V_m$ , the control voltage at the first zero crossing of the phase error, can be found using equations (9) and (14) and numerical iteration. However it is also possible to solve equation (9) in closed form, as shown below.

$$V_m = V_0 \begin{bmatrix} 1 + A(\Lambda_1) \\ + A^2(\Lambda_2) \\ + A^3(\Lambda_3) \\ \vdots \\ + A^{\lfloor \frac{m}{2} \rfloor} \left( \Lambda_{\lfloor \frac{m}{2} \rfloor} \right) \end{bmatrix} \quad (15)$$

Where  $A = -K_V I_P / (F_R^2 C_2)$  and  $\Lambda_1$  up to  $\Lambda_{\lfloor m/2 \rfloor}$  are a set of parameters defined as equations (A1-A5) from appendix A. Since parameter  $|A|$  is always  $\ll 1$ , a further simplification can be made. As  $F_R^2$  is a large number,  $|A|$  becomes less significant as the power of  $A$  is increased. In fact it is found that terms with powers of  $A$  greater than 4 are insignificant and have negligible influence on the final value of  $V_m$ . So (15) can be simplified to:

$$V_m = V_0 [1 + A(\Lambda_1) + A^2(\Lambda_2) + A^3(\Lambda_3) + A^4(\Lambda_4)] \quad (16)$$

Now that the phase error at the zero crossing can be determined, it is possible to determine the stability boundary of the 2<sup>nd</sup> order DPLL using the calculation of the system parameter  $V_m$  in equation (16) and an estimate of  $m$  in (14).

An important system performance criterion is the pull-in rate. Using the system trajectory, as in figure 4 and  $V_m$ , the system pull-in rate can be determined for an initial VCO control voltage offset  $V_0$ .

$$P_{in} = 100 \frac{V_0 + V_m}{V_0} \% \quad (17)$$

If the pull-in percentage is negative, the system is unstable otherwise the system is stable. Combining (16) and (17) the stability criterion can be simplified to:

$$2 + A\Lambda_1 + A^2\Lambda_2 + A^3\Lambda_3 + A^4\Lambda_4 > 0 \quad (18)$$

This is independent of the initial VCO control voltage offset  $V_0$ . As would be expected, the initial condition does not have any effect on the stability boundary. Equating (18) to zero gives the stability boundary of the system and can be compared to the traditional stability boundary of [1].

## IV RESULTS

In figure 7 the stability boundary of the proposed 2<sup>nd</sup> order technique is determined using (18) and is shown along with Gardner's boundary [1] and a stability boundary defined by a circuit level simulation. The accuracy of the circuit level model has been verified using other published behavioural and event driven DPLL models [9-11].

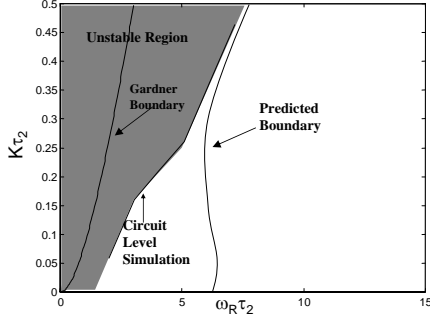


Figure 7. Stability boundaries of 1GHz 2<sup>nd</sup> order PLL according to Gardner and the proposed method.

It is clear from figure 7 that the circuit level model of the DPLL system suggests that Gardner's prediction is insufficiently conservative and does not guarantee stability. In fact there is a significant stable region defined by Gardner, where the circuit level model predicts instability. To emphasise this consider two DPLL systems with a reference frequency of 1GHz, a charge pump gain of  $I_p = 1 \times 10^{-5}$ , and a filter resistor of  $R_2 = 10k\Omega$ . The first DPLL system has  $K\tau_2$  and  $\omega_R\tau_2$  of 0.25 and 10 respectively. From figure 7, this system is expected to be stable as it lies well within the stable region as defined by both models. The output response of this system is determined using a circuit level simulation and is plotted in figure 8.

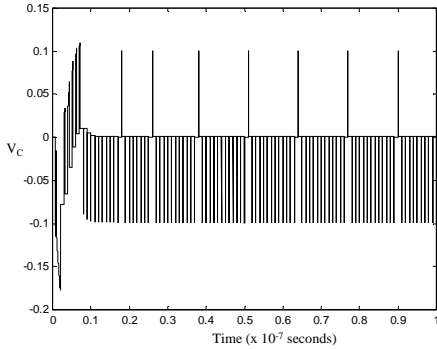


Figure 8. Response of First DPLL System

Ignoring the high frequency jitter, which is inherent to a second order DPLL, this system is stable and settles to an equilibrium after a short period of time. The second system, has  $K\tau_2$  and  $\omega_R\tau_2$  of 0.25 and 2 respectively. Using figure 7, this system is expected to be stable according to Gardner but unstable according to the piecewise linear boundary. The output response of this system is again determined using a circuit level simulation and is plotted in figure 9.

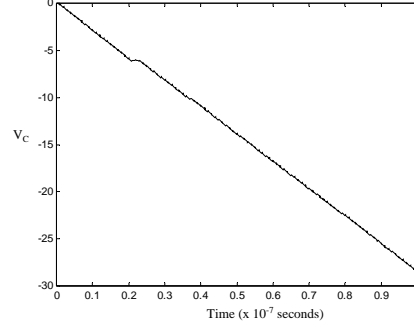


Figure 9. Response of System B

In this case system B is found to be unstable, yet this is counter to Gardner's prediction of stability. This illustrates the inaccuracies of applying the linear model to the DPLL system, as described earlier.

It is clear from figure 7 and the above example that the 2<sup>nd</sup> order piecewise linear technique provides a much better prediction of the stability boundary than linear methods. While comparing the proposed technique to additional stability methods such as [2-4] is desirable, it is not possible due to the specific nature of these methods, and the difficulty in plotting any global stability boundary with such methods.

## V CONCLUSION

Traditional CP-PLL design techniques use linear theory and empirical methods to identify and design stable systems. It is shown in this paper that stability boundaries defined using traditional linear methods are less accurate. The proposed technique uses piecewise linear methods to significantly increase the accuracy of the model relative to existing linear methods, and thus identify more accurate estimates of the stability boundary. This approach considers the exact nonlinear nature of the PFD, rather than simply approximating it to an adder component as in the linear case.

The paper concentrates on the 2<sup>nd</sup> order loop, defining a closed form solution of the stability boundary using linear integration. Though this solution is expansive, it is mathematically tractable and is found to better define the stable region of the DPLL. This technique can be extended to higher orders, however this is beyond the scope of this paper. The resulting model is a significant improvement over existing linear techniques, defining the system stability boundary more accurately for the 2<sup>nd</sup> order of the DPLL.

## VI APPENDIX

### Appendix A – Closed Form Solution of $V_m$

This Section defines the parameters of  $\Lambda$  as used in equations (15), (16) and (18).

$$\Lambda_1 = \begin{bmatrix} 1 \\ 1 \\ 1 \\ \vdots \\ 1 \end{bmatrix}^T \begin{bmatrix} 1 & 0 & 0 & 0 & 0 \\ 1 & b & 0 & 0 & 0 \\ 1 & b & b^2 & 0 & 0 \\ \vdots & \vdots & \vdots & \ddots & 0 \\ 1 & b & b^2 & \dots & b^{n-2} \end{bmatrix} \begin{bmatrix} 1 \\ 1 \\ 1 \\ \vdots \\ 1 \end{bmatrix} \quad (\text{A1})$$

where  $b = I - (K_V R_2 I_P / F_R)$ .

$$\Lambda_2 = \begin{bmatrix} b^{n-4} + 2b^{n-5} + \dots + (n-4)b + (n-3) \\ b^{n-5} + 2b^{n-6} + \dots + (n-5)b + (n-4) \\ \vdots \\ b+2 \\ 1 \end{bmatrix}^T \begin{bmatrix} 1 & 0 & 0 & 0 & 0 \\ 1 & b & 0 & 0 & 0 \\ 1 & b & b^2 & 0 & 0 \\ \vdots & \vdots & \vdots & \ddots & 0 \\ 1 & b & b^2 & \dots & b^{n-4} \end{bmatrix} \begin{bmatrix} 1 \\ 1 \\ 1 \\ \vdots \\ 1 \end{bmatrix} \quad (\text{A2})$$

If we consider  $\Lambda_3$  to be equal to the function  $\Gamma_k$  given in equation (A3) at the bottom of the page, where  $k = 6$ , then  $\Lambda_4$  can be calculated using equation (A4).

$$\Lambda_4 = \begin{bmatrix} \Gamma_8 \\ \Gamma_9 \\ \Gamma_{10} \\ \vdots \\ \Gamma_n \end{bmatrix}^T \begin{bmatrix} 1 & 0 & 0 & 0 & 0 \\ 1 & b & 0 & 0 & 0 \\ 1 & b & b_2 & 0 & 0 \\ \vdots & \vdots & \vdots & \ddots & \vdots \\ 1 & b & b_2 & \dots & b_{n-8} \end{bmatrix} \begin{bmatrix} 1 \\ 1 \\ 1 \\ \vdots \\ 1 \end{bmatrix} \quad (\text{A4})$$

It is possible to calculate all  $\Lambda$  up to  $\lfloor m/2 \rfloor$  by using the same process between equations (A2) and (A4), i.e. define  $\Gamma'_k$  as in equation (A5). Then  $\Lambda_5$  can be calculated as in (A6), and so on up to  $\Lambda_{\lfloor m/2 \rfloor}$

$$\Gamma'_k = \begin{bmatrix} \Gamma_k \\ \Gamma_{k+1} \\ \Gamma_{k+2} \\ \vdots \\ \Gamma_n \end{bmatrix}^T \begin{bmatrix} 1 & 0 & 0 & 0 & 0 \\ 1 & b & 0 & 0 & 0 \\ 1 & b & b_2 & 0 & 0 \\ \vdots & \vdots & \vdots & \ddots & \vdots \\ 1 & b & b_2 & \dots & b_{n-k} \end{bmatrix} \begin{bmatrix} 1 \\ 1 \\ 1 \\ \vdots \\ 1 \end{bmatrix} \quad (\text{A5})$$

$$\Lambda_5 = \begin{bmatrix} \Gamma'_{10} \\ \Gamma'_{11} \\ \Gamma'_{12} \\ \vdots \\ \Gamma'_n \end{bmatrix}^T \begin{bmatrix} 1 & 0 & 0 & 0 & 0 \\ 1 & b & 0 & 0 & 0 \\ 1 & b & b_2 & 0 & 0 \\ \vdots & \vdots & \vdots & \ddots & \vdots \\ 1 & b & b_2 & \dots & b_{n-10} \end{bmatrix} \begin{bmatrix} 1 \\ 1 \\ 1 \\ \vdots \\ 1 \end{bmatrix} \quad (\text{A6})$$

## VII ACKNOWLEDGMENT

The authors acknowledge the support of the Enterprise Ireland commercialisation fund, Science Foundation Ireland and the Centre for Telecommunications Value-Chain Research (CTVR).

## VIII REFERENCES

- [1] Gardner, F.M., "Charge pump phase-lock loops," IEEE Trans. Commun., vol. COM-28, pp1849-1858, Nov 1980.
- [2] Mirabbasi, S., and Martin, K., "Design of Loop Filter in Phase-Locked Loops", IEEE Electronic Letters 1999, Vol. 35, Issue. 21, pp1801-1802
- [3] O'Keese, W., "An Analysis and Performance Evaluation of a Passive Filter Design Technique for Charge Pump PLL's", National Semiconductor Application Note 1001, July 2001
- [4] Williamson, S., "How to Design RF Circuits – Synthesizers", IEE Colloquium on how to Design RF Circuits 2000.
- [5] Abramovitch, D., "Lyapunov Redesign of Classical Digital Phase-Lock Loops", Proceedings of the American Control Conference Denver, Colorado, pp2401-2406, June 2003
- [6] Eva Wu, N., "Analog Phaselock Loop Design Using Popov Criterion", Proceedings of American Control Conf. Anchorage, pp16-18, May 2002
- [7] Rantzer, A., "Almost global stability of phase-locked loops", Proceedings of the 40th IEEE conf. On Decision and control, vol. 1, pp899-900, December 2001
- [8] Simon, D., El-Sherief, H., "Lyapunov Stability Analyses of Digital Phase Locked Loops", IEEE Conference on Systems, Man and Cybernetics, San Antonio, TX, pp2827-2829, October 1994.
- [9] Van Paemel, M., "Analysis of a Charge-Pump PLL: A new Model", IEEE Trans on Communications, VOL.42, No 7, pp2490-2498, July 1994
- [10] Hedayat, C.D., Hachem, A., Leduc, Y., Benhassat, G., "High-level modeling applied to the second-order charge-pump PLL circuit", Texas Instruments Technical Journal, Vol 14, No. 2, March/April 1997
- [11] Hedayat, C.D., Hachem, A., Leduc, Y., Benhassat, G., "Modeling and Characterization of the 3rd Order Charge-Pump PLL: a Fully Event-driven Approach", Analog Integrated Circuits and Signal Processing, vol. 19, pp25-45, April 1999

---


$$\Gamma_k = \begin{bmatrix} b^{n-k} + 2b^{n-k-1} + \dots + (n-k)b + (n-k+1) \\ b^{n-k-1} + 2b^{n-k-2} + \dots + (n-k-1)b + (n-k) \\ \vdots \\ b+2 \\ 1 \end{bmatrix}^T \begin{bmatrix} 1 & 0 & 0 & 0 & 0 \\ 1 & b & 0 & 0 & 0 \\ 1 & b & b^2 & 0 & 0 \\ \vdots & \vdots & \vdots & \ddots & 0 \\ 1 & b & b^2 & \dots & b^{n-k} \end{bmatrix} \begin{bmatrix} 1 \\ 1 \\ 1 \\ \vdots \\ 1 \end{bmatrix} \quad (\text{A3})$$